

Electric-field mapped averaging for the dielectric constant

Weisong Lin, Andrew J. Schultz, David A. Kofke*

*Department of Chemical and Biological Engineering
University at Buffalo, The State University of New York, Buffalo, NY 14260-4200,
U.S.A.*

Abstract

We examine the performance of mapped averaging for the computation of the dielectric constant in application to the TIP4P water potential. We compare the efficiency of conventional and mapped averaging in terms of the difficulty ratio, considering four temperatures (500 K, 650 K, 1300 K, and 1800 K) and densities from 10^{-6} g/cm³ to 1.0 g/cm³. We consider differences in the methods also with respect to correlation of samples, and system-size effects. Results for 650 K are compared to experimental data as represented by a correlation for the dielectric constant from the literature, with deviations of up to 25% observed. Significant advantage in efficiency is seen for the mapped-averaging approach at high temperature and low density, while being marginally less efficient at liquid-like densities. We also examine the simulation data against results from a dielectric virial series to third order in density, and suggest that an even better mapped-averaging method may be developed from consideration of pairwise interactions of the molecular dipoles.

Keywords: molecular simulation, mapped averaging, dielectric constant, TIP4P water

*Author for correspondence.

Email address: kofke@buffalo.edu (David A. Kofke)

1. Introduction

Solution properties have long attracted the attention of researchers in chemical thermodynamics [1, 2, 3, 4]. Molecular models of electrolytes and aqueous solutions rely on a proper treatment of electrostatics for an accurate description of solution behavior. A key property relating to these considerations is the dielectric constant, or relative permittivity. Models of water that aim to be used for studies of solutions should give attention to whether the dielectric constant is predicted well. It characterizes how well a solvent screens the interactions of charges with each other, and thereby has a considerable effect on the general behavior of solutions. Indeed, considerable attention has been given to evaluation of the dielectric properties for various water models via molecular simulation [5, 6, 7, 8]. The dielectric constant is related to the fluctuations in the mean square total dipole moment in the absence of and external electric field [9, 10]. It is considered one of the more difficult properties for calculation by molecular simulation; long-range electrostatic effects are relevant, and like all fluctuation-based quantities, averaging tends to converge slowly.

To aid calculation of precise values of dielectric constant, we developed a formulation of mapped averaging (MA) [11, 12] for its evaluation. Mapped averaging is a new, general method for reformulation of the ensemble averages in statistical mechanics. Given a property approximation based in statistical mechanical theory, the MA framework derives new ensemble averages that represent exactly the error in the theory. If the starting theory is reasonably accurate, the correction given by the averages can be evaluated with good precision, because it eliminates fluctuations related to the known approximate behavior. We have had good success in application of this idea to evaluation of properties of atomic crystals, where a harmonic treatment provides a suitable starting point [13, 14, 12]; the simulations then give directly the anharmonic contributions to properties.

Our application of MA to evaluate the dielectric constant from molecular simulation builds on knowledge of fluctuations in non-interacting dipoles, such that the simulation measures only contributions in excess of this. Presently we consider only rigid, non-polarizable dipoles interacting with an external field \mathbf{E} . When presenting the general MA framework [11], we used application to the dielectric constant as one of several brief examples illustrating the effectiveness of the approach. We performed simulations of the Stockmayer model (Lennard-Jones with point dipole), and showed that MA at low den-

sity yields results that are much more precise than conventional averaging with the same amount of computation.

In this paper, we consider application to a more realistic molecular model, the TIP4P potential for water. This model has three charged sites and one LJ site, which means there are ten pairs of interaction between each pair of molecules, and no explicit dipole-dipole interaction is employed. We examine the effectiveness of MA for such a system. We emphasize calculation of dielectric constant of water in supercritical state. One reason is that most previous simulation studies of the dielectric constant of water considered the liquid state, so we provide new data as a byproduct of the study. Additionally, in the supercritical conditions the non-interacting dipole starting point is more appropriate, and the approach may be anticipated to be more effective. We compare the performance of MA and the conventional approach by consideration of the difficulty. Also we examine other performance-related features that we did not consider in previous work, in particular the rate of decay of correlations, and system-size effects. In applications to the anharmonic behavior of crystals, we found large differences between conventional and mapped averaging with regard to these issues. We also compare our simulation results with experimental data as represented by a correlation.

The formalism and simulation details of MA for calculation of the dielectric constant are presented in Sec. 2 and results are given in Sec. 3. In Section 4, we summarize the findings and consider paths for future development of the MA method for evaluation of the dielectric constant.

2. Formalism and simulation details

2.1. Ensemble averages

We consider molecules with a fixed dipole moment, $|\boldsymbol{\mu}_i| \equiv \mu_D$. The energy of interaction with external field \mathbf{E} is:

$$U_E = -\mathbf{E} \cdot \mathbf{M}, \quad (1)$$

where $\mathbf{M} = \sum_i \boldsymbol{\mu}_i$ is the total dipole moment (here and below, i sums over all N molecules in the system). The dielectric constant is given in terms of the second derivative of the free energy A with respect to the field \mathbf{E} , which yields directly the conventional form for the ensemble average:

$$\nabla_{\mathbf{E}}^2(\beta A) = -\beta^2 (\langle \mathbf{M}^2 \rangle - \langle \mathbf{M} \rangle^2) \quad (2)$$

This is what we will refer to as the conventional averaging approach for evaluating the dielectric constant. For the isotropic and homogeneous systems we consider, there is no permanent dipole moment ($\langle \mathbf{M} \rangle \equiv 0$), so we average just $\langle \mathbf{M}^2 \rangle$.

The MA formulation for this derivative is developed as follows (additional detail is available in Ref. 11). We derive the mapping under an assumption that the probability of a configuration is that for independent dipoles in a z -directed field $\mathbf{E} = (0, 0, E)$. This assumption leads us to define the following:

$$p(\boldsymbol{\Omega}; E) = \exp(-\beta U_E) = \prod_i p_1(z_i; E) \quad (3a)$$

$$p_1(z_i; E) = \exp(\beta \mu_D E z_i) \quad (3b)$$

$$q(E) \equiv \int d\boldsymbol{\Omega} p(\boldsymbol{\Omega}; E) = (q_1(E))^N \quad (3c)$$

$$\begin{aligned} q_1(E) &= \int_{-1}^1 dz_i p_1(z_i; E) \\ &= 2 \sinh(\beta \mu_D E) / (\beta \mu_D E) \end{aligned} \quad (3d)$$

Here, $\boldsymbol{\Omega}$ is the vector of orientations for all N molecules, and z_i is the z -component of the orientation of dipole i . These approximations to the true Boltzmann weight and partition function are used in a type of conservation equation to derive the mapping, which is given via a generalized “rotational velocity” v_i^E (the E superscript indicates that this velocity describes change in orientation with respect to a changing field E , rather than time):

$$\frac{\partial}{\partial E} \left(\frac{p_1(z_i, E)}{q_1(E)} \right) + \frac{\partial}{\partial z_i} \left(\frac{p_1(z_i, E)}{q_1(E)} v_i^E \right) = 0. \quad (4)$$

The mapping given by solution of this formula keeps the ratio p_1/q_1 constant (in the Lagrangian frame) as E is varied. If the independent-dipole approximation is valid, then the formula for the change in free energy with E (as derived below) would be expressed in terms of an average having no fluctuations, yielding a result with perfect precision. To the extent the system does not obey the independent-dipole approximation, there will be fluctuations in the average; however, while some imprecision is introduced, there is no loss of accuracy.

Solution to Eq. (4) with the boundary condition $v^E(z_i = 1) = 0$ yields:

$$v_i^E = \frac{1}{2} \beta \mu_D (1 - z_i^2) \quad (5)$$

The second derivative of the free energy is then [11]:

$$\beta A_{EE} = - \langle J_{EE} - J_E^2 \rangle + \langle \beta U_{EE} \rangle - \text{Var}[J_E - \beta U_E] \quad (6)$$

where subscripts indicate derivatives with respect to E . The Jacobian derivatives are given in terms of the mapping as

$$J_E = \nabla \cdot \mathbf{v}^E, \quad (7a)$$

$$J_{EE} - J_E^2 = \nabla \cdot \mathbf{v}_E^E + \mathbf{v}^E \cdot \nabla(\nabla \cdot \mathbf{v}^E), \quad (7b)$$

and the configurational-energy derivatives are

$$\beta U_E = - \mathbf{M}_z - \mathbf{v}^E \cdot \boldsymbol{\tau} \quad (8a)$$

$$\beta U_{EE} = - (\mathbf{v}_E^E + \mathbf{v}^E \cdot \nabla \mathbf{v}^E) \cdot \boldsymbol{\tau} + \mathbf{v}^E \cdot \boldsymbol{\phi} \cdot \mathbf{v}^E - 2 \mathbf{v}^E \cdot \boldsymbol{\tau}_E, \quad (8b)$$

where $\boldsymbol{\tau}$ is the $3N$ -dimensional vector of the components of the torque on all molecules, and $\boldsymbol{\phi}$ is the $3N \times 3N$ Hessian for the energy with respect to the orientations; also, the ∇ operator here is the $3N$ -dimensional vector of orientation derivatives.

We repeat this derivation for fields in the x and y directions, respectively, and sum over all three directions to obtain the final MA expression for the second derivative [11]:

$$\begin{aligned} \nabla_{\mathbf{E}}^2(\beta A) &= -N\beta^2\mu_D^2 + \frac{\beta^4}{4} \left\langle \left| \sum_{i=1}^N \boldsymbol{\tau}_i \times \boldsymbol{\mu}_i \right|^2 \right\rangle \\ &\quad - \frac{\beta^3}{4} \left\langle \sum_{i=1}^N \sum_{j=1}^N (\nabla_i \cdot \boldsymbol{\tau}_j)(\boldsymbol{\mu}_i \cdot \boldsymbol{\mu}_j) - \boldsymbol{\mu}_j \cdot \nabla_i \boldsymbol{\tau}_j \cdot \boldsymbol{\mu}_i \right\rangle \end{aligned} \quad (9)$$

where $\boldsymbol{\tau}_i$ is the torque on molecule i , and ∇_i is the gradient with respect to the molecule- i orientation. Equation (9) is clearly separated into two parts. The first term in this expression is the Clausius-Mossotti-Debye result [15], which describes fluctuations of independent dipoles. The remaining terms represent the correction to this approximate form, given as ensemble averages that will be small and precise to the extent that the independent-dipole approximation is valid.

Once this derivative is evaluated, the dielectric constant ϵ is obtained, for tin-foil boundary conditions, via [9]:

$$\frac{\epsilon - 1}{3} = -\frac{4\pi}{9V} \nabla_{\mathbf{E}}^2 A, \quad (10)$$

where V is the volume of the simulation cell.

2.2. Simulation details

We performed calculation of the dielectric constant for the TIP4P water potential [16], with a system size of $N = 256$ molecules (except for simulations performed to examine finite-size effects, described below). Constant- NVT Monte Carlo (MC) simulations were performed with 10^8 MC trials, where each trial is an attempted rotation or displacement (50% probability each) of a single randomly selected molecule. Simulations at a few conditions were performed using 10^9 MC trials, specifically: (500 K, 0.4 g/cm³), (500 K, 0.9 g/cm³), (500 K, 1 g/cm³), (650 K, 0.9 g/cm³) and (650 K, 1 g/cm³). Samples were separated into 1000 blocks and the uncertainty was computed as one standard deviation mean of the block averages (68% confidence limits), accounting for block correlations using the method of Kolafa [17]. Simulations were run using the Etomica molecular simulation library [18] on computers with Intel i7-4790s, 3.20GHz CPU. In all cases described below, mapped and conventional averages were computed in separate simulations and the individual timings required to complete a given run were recorded and used to evaluate the difficulty [19] presented here. Interactions were truncated at a distance of 49% of the simulation box-size. The reaction field method was applied to treat the the long-range dipole interactions, using a dielectric constant of the boundary $\epsilon' \rightarrow \infty$ (tin-foil boundary conditions).

We performed calculations from very low densities to values about equal to that of condensed liquid water, and for four temperatures 500 K, 650 K, 1300 K and 1800 K. Some of these are rather extreme conditions, but they are encountered in some natural settings; moreover, we cannot expect the TIP4P model to be accurate at many of these states. Regardless, it is useful to consider a broad range of conditions when evaluating the performance of a method. We note that the critical temperature of (real) water is 647 K, but for the TIP4P model the critical temperature is lower, equal to 588 K [20].

3. Results and discussion

3.1. Difficulty ratio

We first compare the performance of the conventional and MA approaches by examining the difficulty ratio along isotherms and isochores. The difficulty D is defined [19] $D \equiv \sigma t^{1/2}$, where σ is the uncertainty in an average obtained from a simulation requiring CPU time t (conventionally measured in seconds). This group is asymptotically independent of t for sufficiently large t , so it provides a convenient basis for comparison of performance. Note that ratio of CPU times needed to produce a result of the same uncertainty for two different methods is given by the square of the ratio of their difficulties.

The difficulty ratio (conventional/mapped) is plotted for four isotherms in Fig. 1 and five isochores in Fig. 2. In the most extreme case considered here the MA reduces the computational effort by a factor of 10^7 . This occurs at the highest temperature and lowest density—the interaction between dipoles is weakest (relative to $k_B T$) at such conditions, and behavior is closest to the assumption of non-interacting dipoles. On the other hand, while the efficiency is high at these conditions, the correction to the Clausius-Mossotti-Debye estimate is correspondingly small, so the quantity being averaged is increasingly unimportant. For the low temperature and high density region, the MA is seen to be slightly less efficient (difficulty ratio between 0.9 and 1, and lower in a few cases), but it is no less accurate. Between these extremes, the MA approach provides a useful level of computational speedup, perhaps halving or more the amount of CPU required to obtain a result to a given precision. Thus, the MA could be used for all of the supercritical region without concern for incurring any disadvantage and, assuming it is implemented in code, there is little reason to avoid using it to calculate the dielectric constant.

3.2. Correlation

Studies of MA in application to crystal properties found considerable advantage with respect to the decay of correlations in the quantity being averaged [12]. A quickly-decaying autocorrelation corresponds to effectively more independent data, and contributes to a smaller uncertainty for a given amount of total sampling. We examine the dielectric MA in this respect, and consider the quantity [21]:

$$s \equiv M \frac{\sigma_X^2(b)}{\sigma_X^2}. \quad (11)$$

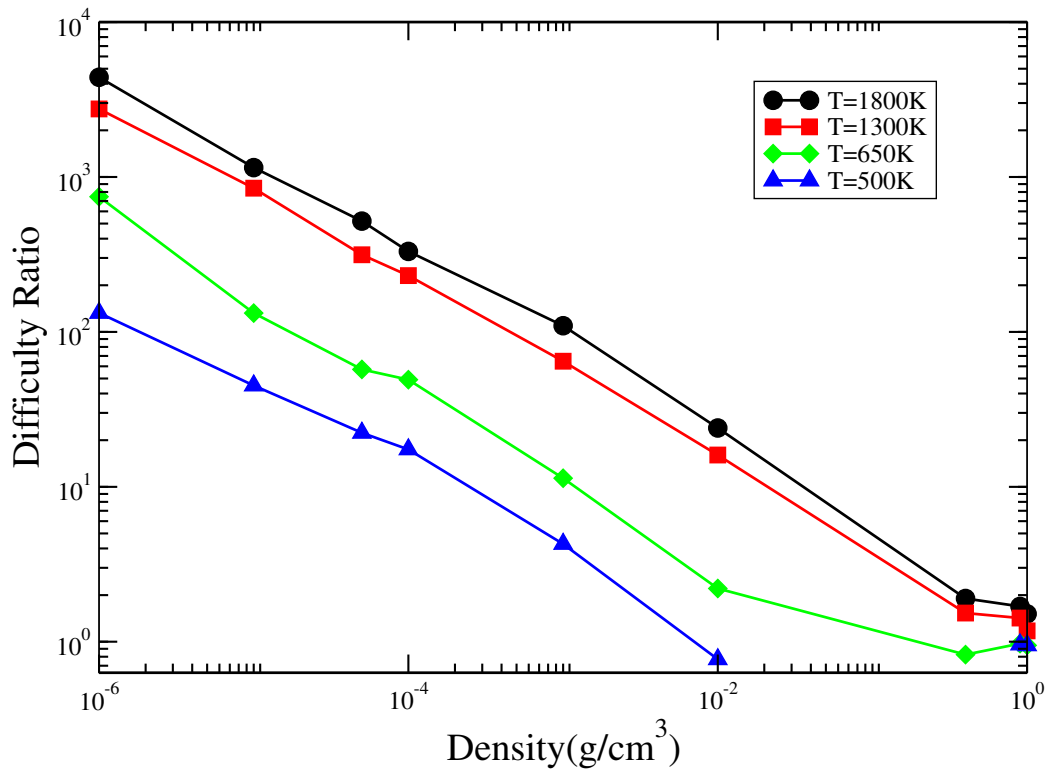


Figure 1: Difficulty ratio $D(\text{conventional})/D(\text{mapped})$, for calculation of the dielectric-constant derivative $\nabla_{\mathbf{E}}^2(\beta A)$, computed for the TIP4P water potential along the four isothermal lines. Data for $T = 500$ K extend into the two-phase region beyond its saturation density (equal to 0.013 g/cm^3 for real water). Straight lines join the points as a guide to the eye.

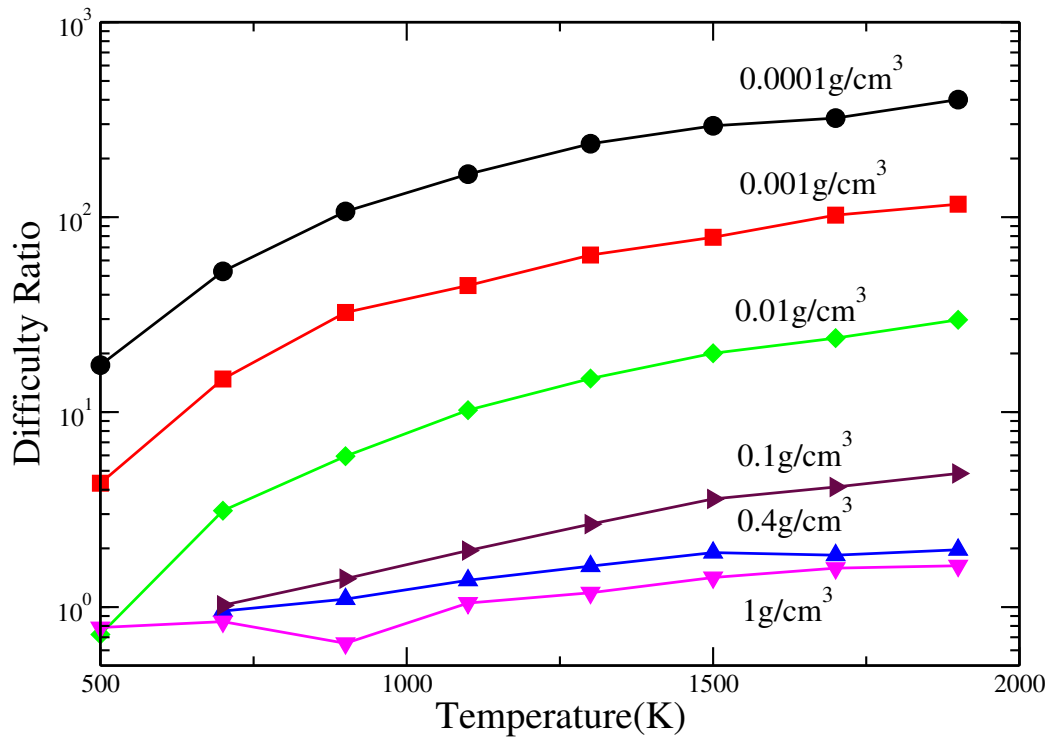


Figure 2: Difficulty ratio for mapped versus standard averaging of the dielectric-constant derivative $\nabla_{\mathbf{E}}^2(\beta A)$, computed for the TIP4P water potential along the five isochores. Datum for 0.4 g/cm³ is not shown in its vapor-liquid coexistence region. Straight lines join the points as a guide to the eye.

Here, M is the total number of MC steps performed in the simulation, and σ_X^2 is the variance of the sampled values (denoted X , which represents the right-hand side of Eq. (2) or (9) for conventional and MA, respectively). The variance of the mean $\sigma_X^2(b)$ is obtained as the variance of subaverages of blocks of b samples each, divided by the number of blocks (equal to M/b). In general, s depends on block size for small b , but becomes asymptotically independent of b for sufficiently large blocks; this is the value of s that is of interest.

The quantity s can be interpreted as the number of samples required to obtain an independent block average. If each configuration were independent of the previous one, then we would have $s = 1$, but in practice the MC method generates highly correlated configurations, and it takes many samples to generate an independent block average. There is advantage in requiring fewer samples to generate an independent block average, because it allows a given number of samples to provide effectively more data. Interestingly, s depends on the property being computed and the method of calculation, and this is what we examine now.

Figure 3 presents a comparison of s for data at one temperature and two densities, comparing conventional and MA. Considering first the liquid density, we see that conventional averaging requires almost 10 times more samples to generate an independent block, compared to MA. The MA method already accounts for fluctuations involving large variations in the orientations of the dipoles, and instead it requires averages that depend on the intermolecular interactions, which can decorrelate more quickly than fluctuation in the total dipole moment. The situation is switched and less extreme at the low-density example. Here the conventional average decorrelates about twice as fast as the mapped average. The relative independence of the dipoles allows fast decorrelation of \mathbf{M} , while the long-range interactions contribute to longer correlation of the relevant quantities for MA.

Notably, s is not alone in determining the efficiency of the calculation. Even with the faster decorrelation for MA, at liquid densities both approaches are roughly equal in efficiency (cf. Figs. 1 and 2); this may reflect in part the extra computational cost required for MA, which is included in the difficulty ratio. Then, despite its slightly slower decorrelation, at the vapor density the MA is vastly superior, reflecting the much smaller size of the fluctuations that give rise to the uncertainty in its average.

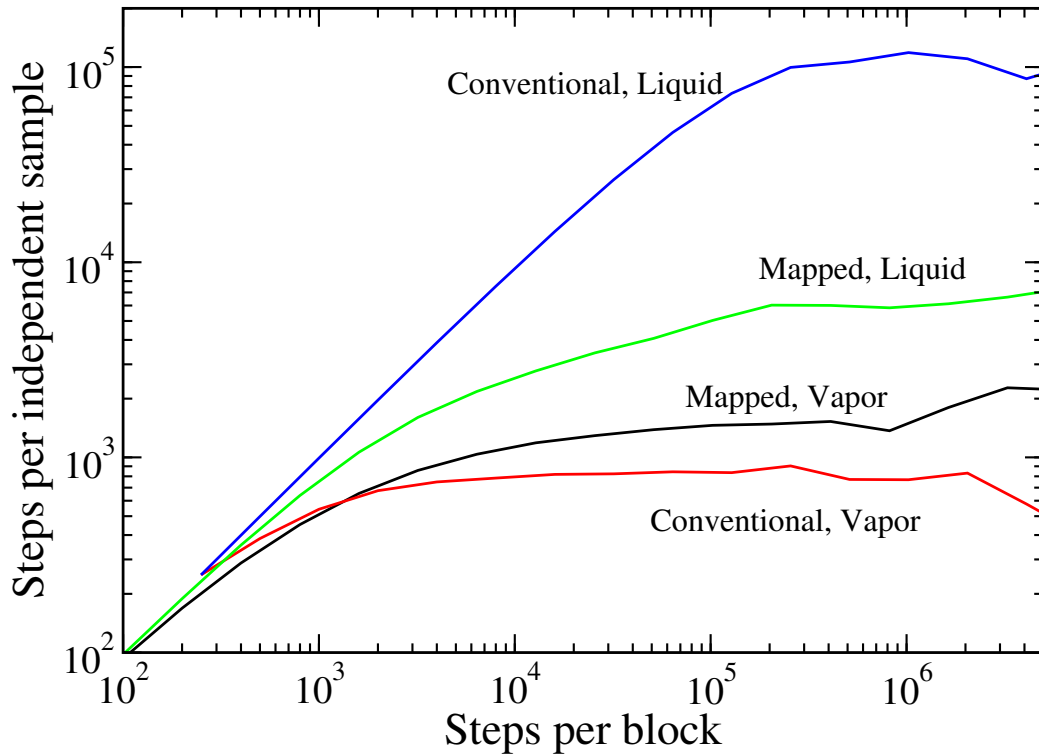


Figure 3: The number of MC steps needed to obtain an effectively independent sample (s , as defined in Eq. (11)), as a function of the number of steps per block, b . Results are presented for averages taken conventionally (Eq. (2)) and using the mapping (Eq. (9)), as indicated. Results labeled “liquid” are for 0.9 g/cm^3 , and “vapor” are at 0.001 g/cm^3 . All data are for 650 K .

3.3. System size effect

For crystals, mapped averaging also shows considerable advantage with respect to finite-size effects [12]. The anharmonic contributions computed directly by the simulation are essentially independent of the system size, while the accuracy of the harmonic component is significantly affected, with the consequence that small-system results taken by conventional averaging are compromised. To investigate this issue for the dielectric-constant calculation, we evaluated $\nabla_{\mathbf{E}}^2(\beta A/N)$ via simulations of $N = 100, 200, 400, 800$ and 1600 molecules, respectively. As with the analysis of correlations, we consider one low and one high density: 0.001g/cm^3 and 0.9 g/cm^3 , both at $T = 650\text{ K}$. Data are plotted in Figs. 4 and Fig. 5. The figures show that the lines of $\nabla_{\mathbf{E}}^2(\beta A/N)$ are in all cases practically horizontal for both methods, indicating that both MA and conventional method are insensitive to system-size effects. We also notice that the uncertainty of MA is always smaller than that of the conventional average, especially at the lower density, demonstrating that the MA is more precise than the conventional with same MC steps.

Turning from the issue of accuracy, let us examine the effect of system size on relative precision of the methods. This is presented again in terms of the difficulty ratio, shown in Fig. 6 as a function of (inverse) system size. For 0.9 g/cm^3 density, the MA and the conventional average basically have the same difficulty, with the ratio fluctuating between 0.95 and 1.3 across the system sizes. At the lower density of 0.001 g/cm^3 , the advantage of the MA increases with increasing system size. One can reason that the relative uncertainty ($\mathcal{R}_X \equiv \delta_X/X$, where δ_X is the uncertainty of X) of the conventional average $\langle \mathbf{M}^2 \rangle$ is proportional the square root of N [22, 23] ($\mathcal{R}_{\mathbf{M}^2} \propto \sqrt{N}$), which is consistent with our data (not shown) for conventional averaging. For the MA in Eq. (9), there are three components: $-N\beta^2\mu_D^2$, and two averages. The first component is given exactly, hence its uncertainty is zero. The second component (involving $\boldsymbol{\tau}_i \times \boldsymbol{\mu}_i$) is a square of an extensive quantity, which has the same behavior as $\langle \mathbf{M}^2 \rangle$, i.e. ($\mathcal{R} \propto \sqrt{N}$). The third component is just an extensive average and its relative uncertainty is independent of system size. In the case of density 0.9 g/cm^3 , the second component of MA becomes dominant and the difficulties of the MA and the conventional are close to each other. Hence, the difficulty ratio plot is almost horizontal with value near unity for this density. In the case of density 0.001g/cm^3 , the second component becomes less important and the relative uncertainty of MA decreases with increasing system size, leading to an increase in difficulty ratio for this density. So the MA tends to have results with smaller uncertainty

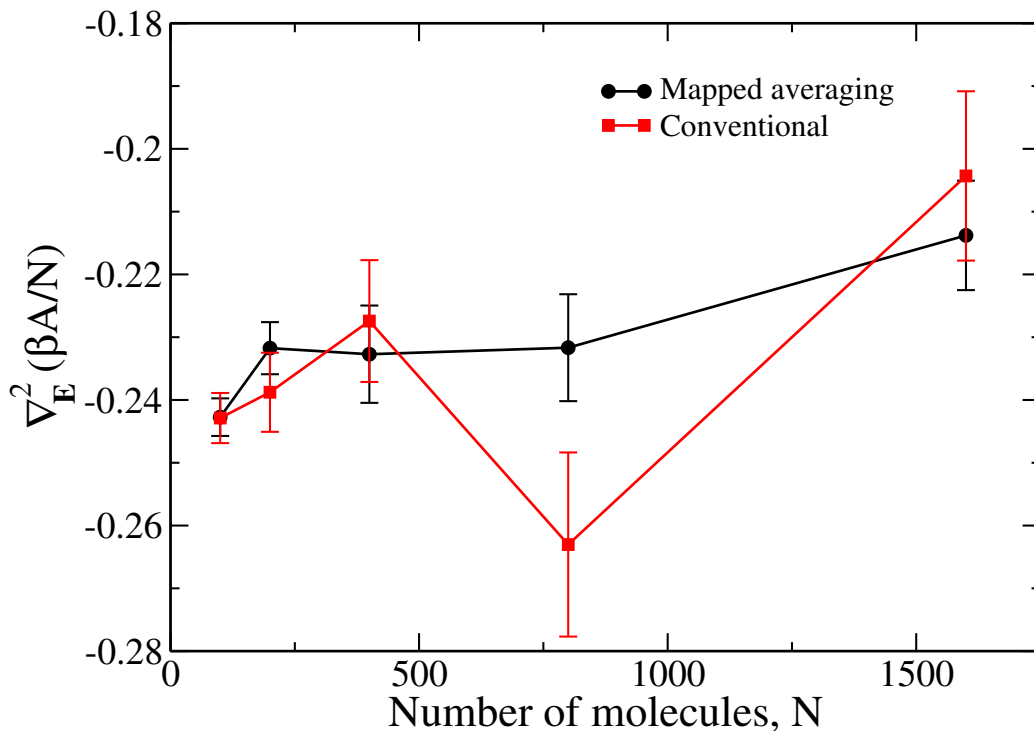


Figure 4: Comparison of system-size effects of MA and conventional methods for $T = 650$ K, $\rho = 0.9$ g/cm³. The error bars indicate the 68% uncertainty estimates of the data.

than that of the conventional average for large systems in supercritical states.

3.4. Comparison between correlation and simulation data

Lastly, we compare the MA simulation data to experiment as represented by the empirical correlation of Fernández [24]. Comparison is presented in Fig. 7 for the 650 K isotherm (the correlation is valid only up to 873 K, so we do not consider higher temperatures). The results for the MA and the conventional average are indistinguishable on this scale, so we present only the MA results. Inasmuch as it is non-polarizable, TIP4P water is unrealistic, so it is not surprising that the simulation data does not match the correlation plot perfectly. In particular, the simulation results overestimate the dielectric constant for the low-density region (as expected for a fixed-charge model parameterized for the liquid) and underestimates for the high-density region. As shown by the inset figure, the differences are about 25% for the two cases.

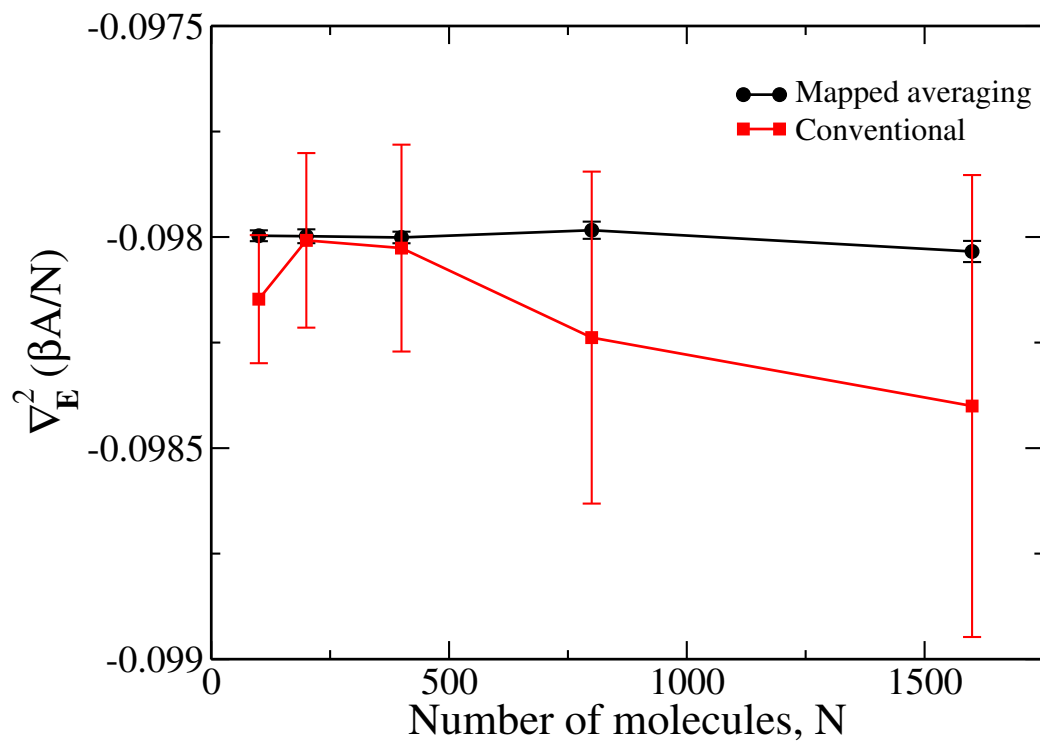


Figure 5: Comparison of system-size effects MA and conventional methods for $T = 650$ K, $\rho = 0.001$ g/cm³. The error bars indicate the 68% uncertainty estimate of the data.

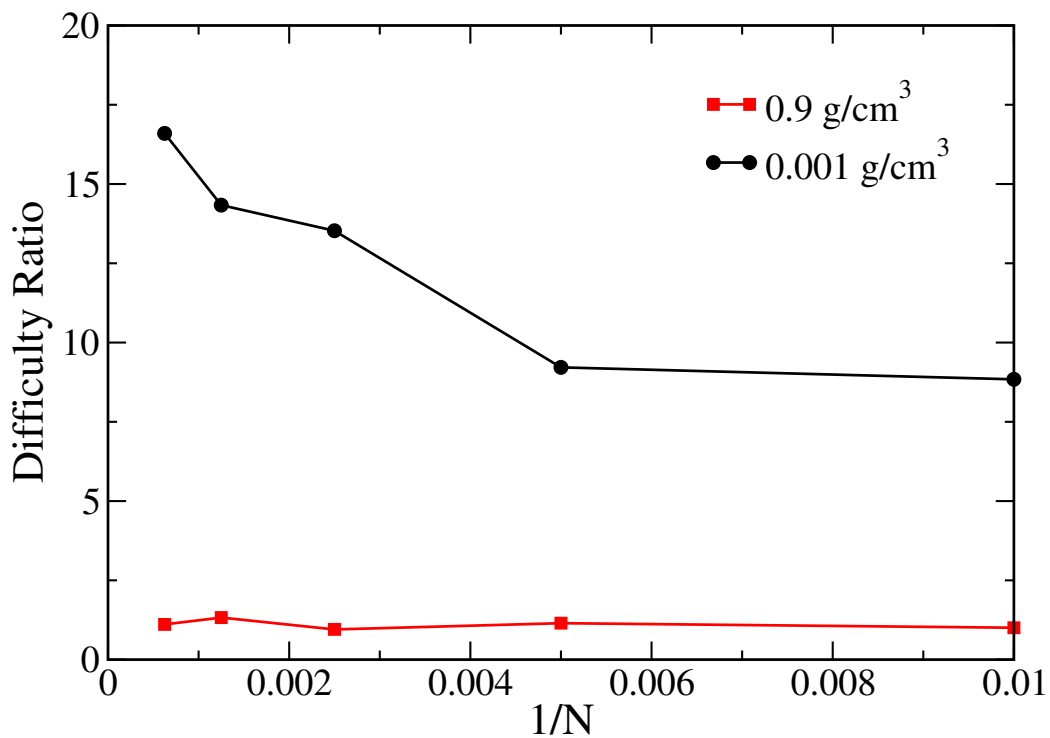


Figure 6: Difficulty ratio for mapped versus standard averaging of the dielectric-constant derivative $\nabla_{\mathbf{E}}^2(\beta A)$, computed for the TIP4P water potential for two densities at 650 K. The abscissa is system size given as $1/N$, so larger systems are toward the left.

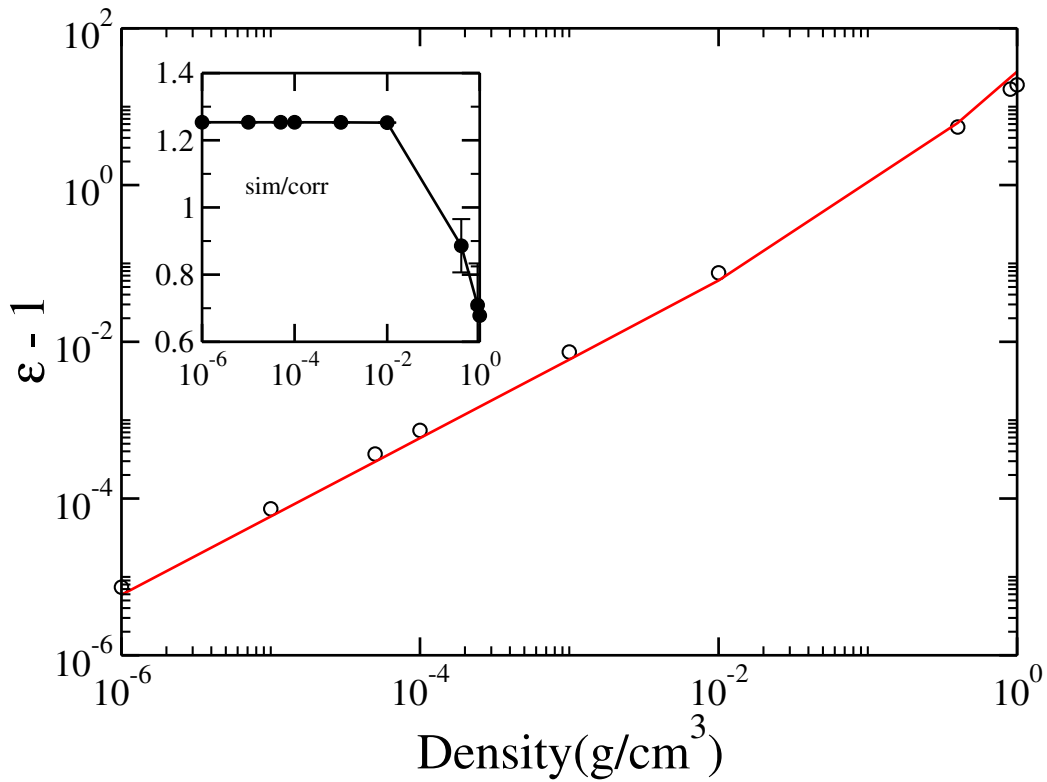


Figure 7: Dielectric constant of water (given as $\epsilon - 1$) at 650 K as a function of density, comparing an empirical correlation [24] based on laboratory measurements of real water (red line), and simulation data for the TIP4P model of water (circles, showing results of mapped-average calculations, with uncertainties smaller than symbol size). Inset shows the $(\epsilon - 1)$ ratio, (simulation data)/(correlation).

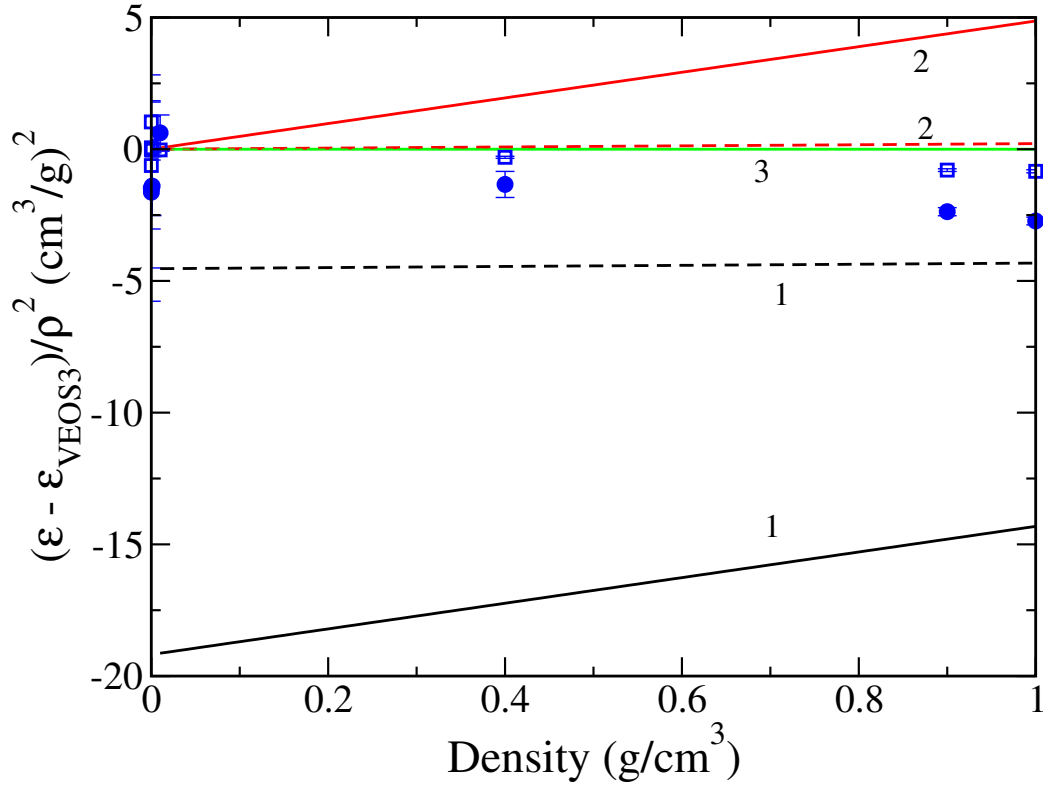


Figure 8: Comparison of the dielectric constant given by molecular simulation (points) to estimates from the dielectric virial series [25], for two temperatures: 650 K (filled circles, solid lines); and 1300 K (open squares, dashed lines). Data are presented as differenced from the 3rd-order virial series (VEOS3), and divided by ρ^2 to accentuate the differences at low density (in this representation, VEOS1 is not zero at its intercept). Numerals next to each line indicate the order of the dielectric virial series.

4. Conclusion

We have applied a mapped-averaging framework to compute the dielectric constant of TIP4P water for the non-condensed vapor and supercritical states, and compared the results with conventional averaging. Results demonstrate that the MA can save computational effort, potentially many orders of magnitude in favorable conditions, while in the worst cases the reformulated averages are just slightly slower to converge. The calculations are most useful in examining deviations from the Clausius-Mossotti-Debye approximation at low-to-moderate densities.

The MA formulation employed here is especially useful if high-precision values of the dielectric constant are required at low density. Such an application may arise if attempting to generate data from first-principles quantum chemistry methods, which could be of interest for generating standard property data that aim to exceed the accuracy possible from experimental measurements.

Mapped averaging is a general means to reformulate ensemble averages, and it is possible to develop other formulations of the approach beyond that considered here. The effectiveness of a MA depends on how well the approximation it is built upon describes the system at the conditions of interest. It is possible, for example, to develop a MA formulation based on pairwise interactions of the dipoles, rather than a treatment based on independent dipoles. Such an approach would yield an expression for $\nabla_{\mathbf{E}}^2(\beta A)$ that again begins with the first-order (in density) Clausius-Mossotti-Debye term, then adds a second-order term with coefficient that is similar to a dielectric second virial coefficient; the remaining terms would be ensemble averages that yield directly the error in the second-order approximation. In recent studies of the dielectric virial series [25], we found that the second-order expansion performs very well in comparison to simulation, and improves significantly on the first-order treatment. This is demonstrated for the TIP4P system in Fig. 8 (using dielectric virial coefficients computed here for this purpose). This observation suggests that it would be worthwhile to pursue development of the dielectric MA with a pairwise-dipole-interaction starting point.

Acknowledgement

This work was supported by the U.S. National Science Foundation, grant CBET-1510017.

5. References

- [1] A. V. Plyasunov, E. L. Shock, J. P. O’Connell, Corresponding-states correlations for estimating partial molar volumes of nonelectrolytes at infinite dilution in water over extended temperature and pressure ranges, *Fluid Phase Equil.* 247 (1-2) (2006) 18–31.
- [2] J. P. O’Connell, R. Gani, P. M. Mathias, G. Maurer, J. D. Olson, P. A. Crafts, Thermodynamic Property Modeling for Chemical Process and Product Engineering: Some Perspectives, *Ind. Eng. Chem. Res.* 48 (10) (2009) 4619–4637.
- [3] D. Dolejs, Thermodynamics of Aqueous Species at High Temperatures and Pressures: Equations of State and Transport Theory, in: Stefansson, A and Driesner, T and Benezeth, P (Ed.), *Thermodynamics of Geothermal Fluids*, Vol. 76 of *Reviews in Mineralogy & Geochemistry*, 2013, pp. 35–79, 23rd Annual VM Goldschmidt Conference, Florence, ITALY, AUG 24-25, 2013. doi:10.2138/rmg.2013.76.3.
- [4] R. Wedberg, J. P. O’Connell, G. H. Peters, J. Abildskov, Total and direct correlation function integrals from molecular simulation of binary systems, *Fluid Phase Equil.* 302 (1-2, SI) (2011) 32–42.
- [5] M. Neumann, Dielectric relaxation in water. Computer simulations with the TIP4P potential, *J. Chem. Phys.* 85 (3) (1986) 1567–1580.
- [6] J. Anderson, J. J. Ullo, S. Yip, Molecular dynamics simulation of dielectric properties of water, *J. Chem. Phys.* 87 (3) (1987) 1726–1732.
- [7] H. E. Alper, R. M. Levy, Computer simulations of the dielectric properties of water: Studies of the simple point charge and transferrable intermolecular potential models, *J. Chem. Phys.* 91 (2) (1989) 1242–1251.
- [8] T. Simonson, Accurate calculation of the dielectric constant of water from simulations of a microscopic droplet in vacuum, *Chem. Phys. Lett.* 250 (5) (1996) 450 – 454.
- [9] M. Neumann, Dipole moment fluctuation formulas in computer simulations of polar systems, *Mol. Phys.* 50 (4) (1983) 841–858.

- [10] M. Neumann, O. Steinhauser, On the calculation of the dielectric constant using the Ewald-Kornfeld tensor, *Chem. Phys. Lett.* 95 (4) (1983) 417 – 422.
- [11] A. J. Schultz, S. G. Moustafa, W. Lin, S. J. Weinstein, D. A. Kofke, Reformulation of ensemble averages via coordinate mapping, *J. Chem. Theory. Comput.* 12 (4) (2016) 1491—1498.
- [12] S. G. Moustafa, A. J. Schultz, D. A. Kofke, Very fast averaging of thermal properties of crystals by molecular simulation, *Phys. Rev. E* 92 (2015) 043303.
- [13] S. G. Moustafa, A. J. Schultz, D. A. Kofke, Harmonically Assisted Methods for Computing the Free Energy of Classical Crystals by Molecular Simulation: A Comparative Study, *J. Chem. Theory Comput.* 13 (2) (2017) 825–834.
- [14] S. G. Moustafa, A. J. Schultz, D. A. Kofke, A comparative study of methods to compute the free energy of an ordered assembly by molecular simulation, *J. Chem. Phys.* 139 (2013) 084105.
- [15] D. W. Jepsen, Calculation of the Dielectric Constant of a Fluid by Cluster Expansion Methods, *J. Chem. Phys.* 44 (2) (1966) 774.
- [16] C. Vega, J. L. F. Abascal, I. Nezbeda, Vapor-liquid equilibria from the triple point up to the critical point for the new generation of tip4p-like models: Tip4p/ew, tip4p/2005, and tip4p/ice, *J. Chem. Phys.* 125 (3) (2006) 034503.
- [17] J. Kolafa, Autocorrelations and subseries averages in Monte Carlo Simulations, *Mol. Phys.* 59 (5) (1986) 1035–1042.
- [18] A. J. Schultz, D. A. Kofke, Etomica: An object-oriented framework for molecular simulation, *J. Comput. Chem.* 36 (2015) 573–583.
- [19] A. J. Schultz, D. A. Kofke, Quantifying computational effort required for stochastic averages, *J. Chem. Theory Comput.* 10 (2014) 5229–5234.
- [20] C. Vega, J. Abascal, I. Nezbeda, Vapor-liquid equilibria from the triple point up to the critical point for the new generation of TIP4P-like models: TIP4P/Ew, TIP4P/2005, and TIP4P/ice, *J. Chem. Phys.* 125 (3) (2006) 034503.

- [21] M. P. Allen, D. J. Tildesley, *Computer Simulation of Liquids*, Oxford University Press, New York, 1987.
- [22] H. Flyvbjerg, H. G. Petersen, Error estimates on averages of correlated data, *J. Chem. Phys.* 91 (1) (1989) 461–466.
- [23] K. Shaul, A. Schultz, A. Perera, D. Kofke, Integral-equation theories and mayer-sampling monte carlo: a tandem approach for computing virial coefficients of simple fluids, *Mol. Phys.* 109 (20) (2011) 2395–2406.
- [24] D. P. Fernández, A. R. H. Goodwin, E. W. Lemmon, J. M. H. Levelt Sengers, R. C. Williams, A Formulation for the Static Permittivity of Water and Steam at Temperatures from 238 K to 873 K at Pressures up to 1200 MPa, Including Derivatives and Debye–Hückel Coefficients, *J. Phys. Chem. Ref. Data* 26 (4) (1997) 1125–1166.
- [25] S. Yang, A. J. Schultz, D. A. Kofke, Evaluation of second and third dielectric virial coefficients for non-polarisable molecular models, *Mol. Phys.* 115 (8) (2017) 991–1003.